NUMERICAL AND EXPERIMENTAL STUDY ON PLATE FORMING USING THE TECHNIQUE OF LINE HEATING

(DOI No: 10.3940/rina.ijme.2014.a3.301)

B Zhou, **X Han**, and **S-K Tan**, Maritime Research Centre, Nanyang Technological University, Singapore, **Y Liu** and **Z Wei**, Department of Naval Architecture, Dalian University of Technology, China

SUMMARY

Nowadays manual and experiential technique patterns of line heating process could not meet the requirement of modern shipbuilding. Therefore, the automatic forming method is being an active research topic in manufacturing. An accurate and practical predicting method is an essential part of the automatic plate forming system. In the present work a numerical elasto-plastic thermo-mechanical model has been developed for predicting the thermal history and resulting deformation and residual stress field of line heating process. A moving Gaussian distributed heat source was used in the modelling to create a realistic simulation of the process. The transient temperature distributions were predicted using temperature-dependent material properties. The deformation and residual stress field were predicted based on the transient temperature distributions of line heating. Experiments were conducted to prove the validity of the numerical thermo-mechanical model. The final numerical results of temperature, deformation and residual stresses are in good agreement with experiment results. The proposed method presents a valuable reference for the study of similar thermal process.

NOMENCLATURE

A_c	The cross-sectional area of the cutting line
α	Thermal diffusivity
b	Heat transfer coefficient, $b = 2a / c\rho h$
c	Specific heat
dt	The time for each load step
Dλ	The ratio parameter
h	Plate thickness
H_{Fe}	Combustion heat of steel
H_G	The heat generation rates of each load step
k	Thermal conductivity
K	Width factor of Gaussian distribution, $K = \frac{3}{r_0^2}$
K_0	Bessel function, 2nd kind and zero order
$q(r)$	Heat flux from heating torch as a function of r
q_M	Peak value of Gaussian distributed heat flux
Q	Heat input
Q_r	Total heat flux from torch to plate
r	Distance from centre of heat source
r_0	Radius of the gas torch
R_r	The radiation constant
t	Time
T	Temperature
T_0	The initial temperature, set as 20 degree centigrade
T_{m1}	Melting temperature of ferric oxide
T_v	Combustion heat of propylene gas
T_z	The absolute zero on the temperature scale used
v	Processing speed
w	The width of cut slit
β	The heat transfer coefficient
η	Thermal efficiency of propylene gas
η_{Fe}	Thermal efficiency of steel
λ	Thermal conductivity
ρ	Density of steel

1. INTRODUCTION

The line heating method is a popular and efficient technique for forming the ship hull pieces, cars, airplanes, and other complex curved objects. Traditionally, the double-curved plate forming in most shipyards depends on the experience of skilled workers and requires many man-hours. These manual and experiential techniques patterns of line heating have become a bottle-neck in the modern production of shipbuilding. Over the past decades, automation of the line-heating process becomes an active research topic in the shipbuilding industry. It is believed that by drawing on the experience of computer and numerical control techniques, geometric analysis, line heating parameters prediction, plate automatic inspection and reprocessing, automation of the plate-forming process could be achieved.

Moshaiov et al. (1987), Ji et al. (2001) and Ueda K. (1994) conducted studies on the mechanism of the line heating process to predict the final shape of the metal plate according to the heating conditions and mechanical properties of the plate. Some simplified beam or plate theory are usually applied. Jong et al. (2003) typically performed heat transfer analysis between a heat source and the steel plate to determine the temperature field.

Different heat sources for line heating process included gas torch, laser beam (See Kyrsanidi AK, 1999), welding arc (Kitamura et al., 1996) and high-frequency induction heating (see Ogawa J., 2003). Gas torch is the cheapest to maintain and are readily available in most shipyards. Most studies for line heating have been reported by using gas torch. However, the heat input intensity is difficult to control and repeatability is not readily achievable.

The process of plate forming by line heating is a typical coupled and non-linear thermo-mechanical process. Many numerical thermal-elastic-plastic analyses for line heating have been reported. Moshaiov et al. (1991) investigated the unsteady temperature field in the plate during a flame bending process set in the transient analysis mode. Jang et al. 1997 proposed a thermal elastic-plastic analysis model, which uses springs to represent the interactions between the central plastic area and the surrounding elastic areas. In addition, the heat flux from line heating is treated as a point source, which

results in considerable errors in predicting the temperature field. Yu et al. (2001) presented a three-dimensional thermo-mechanical model for the prediction of angular deformations of metal plates due to line heating. The disadvantages of the full three-dimensional models is that the computation time required is typically very long, in terms hours to days, see Yu et al. (1999 and 2000). Wang et al (2006a) apply a new forced convection boundary condition for the numerical simulation of line-heating process.

Some researchers studied the line heating process of based on the experience. Ueda K. (1994) and Liu et al. (2006) designed the proper heating and cooling processes based on the experience of forming simple shape surfaces from rectangular plates. Strain or curvature analysis is employed to determine heating lines.

Shin et al. (2003) and Liu et al. (2006) reported study on line heating process using computer-aided control system. The main function of the computer-aided control system is to provide real-time heating information to automated machines. The machine provides automated line-heating tasks and collects relevant information during and after the task. This information includes, among others, heating location, torch speed and heating sequence.

The objective of this paper is to develop a method to predict the thermal history and resulting deformation and residual stress field of line heating process. To achieve this objective, a numerical elasto-plastic thermo-mechanical model is developed for the line heating process. The results of the analysis were compared with the experimental results to validate the usefulness and effectiveness of the proposed method.

2. THEORETICAL BACKGROUNDS

2.1 THE MECHANISM OF LINE HEATING PROCESS

Line heating is a method of forming double-curve plates by means of local heat treatment. Figure 1 shows conventional line heating work using oxyacetylene torch and water hoses as the main tools. When the plate is subjected to local heating, two things happen: the material becomes softer (lower yield limit) and at the same time it expands. The adjacent material still has its original strength, why the hot and soft steel will yield and make the plate slightly thicker. Upon water cooling the material will regain its strength and the thermal contraction bends/shrinks the plate. This mechanism is illustrated in Figure 2, see Yu (2000).

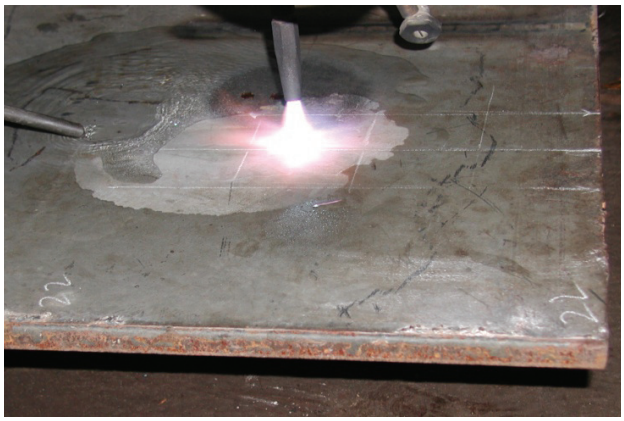

Figure 1. Line heating process on flat plate

2.2 TEMPERATURE FIELD ANALYSIS

Heat flux from an oxyacetylene torch may be described by the Gaussian distribution (Figure 3), see Rykalin (1960) and has been adopted among others such as Moshaiov et al. (1991) and Shin et al. (2003). Taking the center of heat source as the origin of coordinates, the Gaussian distribution is expressed as

$$q(x,y) = q_M \cdot \exp[-K(x^2 + y^2)] = q_M \exp[-Kr^2] \quad (1)$$

where $q(x,y)$ is heat flux density of point (x, y) [J/m^2·s]. q_M, is the peak value of heat flux density (shown in Figure 1) [J/(m^2·s)], expressed as

$$q_M = \frac{\eta \cdot Q \cdot T_v \cdot K}{3600\pi} \quad (2)$$

The total heat input, Q_r, is calculated as the integral of the distribution:

$$Q_r = \int_0^{2\pi} \int_0^{\infty} qrdrd\theta = \frac{\pi q_M}{K} \quad (3)$$

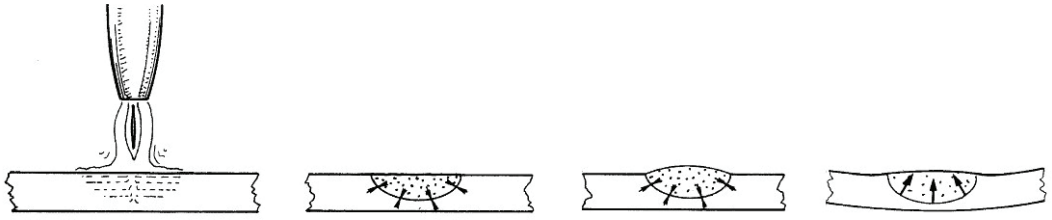

Figure 2. The mechanism of line heating

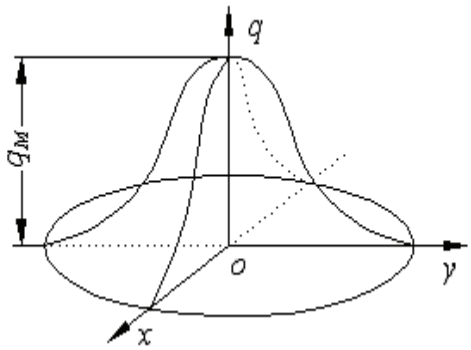

Figure 3. Flux density distribution of Gauss model

The line heating temperature field is a typical of nonlinear and unsteady transient heat conduction problem. The temperature T (t, x, y, z) as a function of time (t) and spatial coordinates (x, y, z) satisfies the following diffusion equation at every point within a finite domain (see Rosenthal D., 1946).

$$c\rho\frac{\partial T}{\partial t}=\frac{\partial}{\partial x}(\lambda\frac{\partial T}{\partial x})+\frac{\partial}{\partial y}(\lambda\frac{\partial T}{\partial y})+\frac{\partial}{\partial z}(\lambda\frac{\partial T}{\partial Z})+Q \qquad (4)$$

Boundary heat transfer is modeled based on natural heat convection and radiation. The convection equation is based on Newton's law of motion, where the coefficient of convective heat transfer is a function of the temperature difference between the boundary and the environment and of the orientation of the boundary.

And the solution of a moving circular area heat source on the semi-infinite body, see Radaj (1992), is given by

$$T-T_0=\frac{2Q}{vc\rho}\cdot\frac{\exp(-\frac{z^2}{4at})}{(4\pi at)^{1/2}}\cdot\frac{\exp(-\frac{r^2}{4a(t+t_0)})}{[4\pi a(t+t_0)]^{1/2}} \qquad (5)$$

Substituting Eq.(3) into Eq.(5), the temperature of the metal combustion process is expressed as

$$T-T_0=\frac{2\pi q_M}{Kvc\rho}\cdot\frac{\exp(-\frac{z^2}{4at})}{(4\pi at)^{1/2}}\cdot\frac{\exp(-\frac{r^2}{4a(t+t_0)})}{[4\pi a(t+t_0)]^{1/2}} \qquad (6)$$

2.3. DEFORMATION FIELD ANALYSIS

For deformation field analysis of steel plate, in case of knowing the temperature field at any moment t, the corresponding displacement field, strain field and stress field satisfy the following equations.

2.3 (a) Strain-displacement equations

As we know, the high temperature is limited in a narrow area which is below 30mm. The temperature difference between both sides of steel plate is more than 400°C. The thickness of steel plate is normally more than 10mm. The thermal expansion coefficient is taken as 1.5X10-5/°C. It could be estimated that the Nonlinearity parts are less than 10^{-2}, which could be ignored. So Strain-displacement equations is as below

$$\varepsilon_{ij}=\frac{1}{2}(u_{i,j}+u_{j,i}) \qquad (7)$$

2.3 (b) Stress-strain equations

In line heating process, once yield occurs, the steel plate will deform plastically. When examining the strains in a plastic material, it should be emphasized that one works with increments in strain rather than a total accumulated strain, as the temperature field is transient and complex. As the elastic strain is not as small as to be negligible, the Stress-strain equations of line heating are set up based on the Prandtl-Reuss equations.

The total strain can be decomposed into an elastic part and a plastic part.

$$\varepsilon_{ij}=\varepsilon_{ij}^{e}+\varepsilon_{ij}^{p}$$

The corresponding Strain increment is shown as below

$$d\varepsilon_{ij}=d\varepsilon_{ij}^{e}+d\varepsilon_{ij}^{p}$$

The Elastic strain increment is

$$d\varepsilon_{ij}^{e}=\frac{1+v}{E}d\sigma_{ij}-\frac{v}{E}d\sigma_{kk}\delta_{ij}$$

The plastic strain increment is

$$de_{ij}^{p}=s_{ij}d\lambda$$

$d\lambda$ is the ratio parameter.

So that the Stress-strain equations is

$$d\varepsilon_{ij}=\frac{1+v}{E}d\sigma_{ij}-\frac{v}{E}\delta_{ij}d\sigma_{kk}+s_{ij}d\lambda \qquad (8)$$

2.3 (c) Equilibrium equations

Utilizing Newton's second law and the graphical representation of the state of stress, the following equilibrium equations are given.

$$\begin{aligned}&\frac{\partial\sigma_{xx}}{\partial x}+\frac{\partial\sigma_{yx}}{\partial y}+\frac{\partial\sigma_{zz}}{\partial z}=0\\&\frac{\partial\sigma_{xy}}{\partial x}+\frac{\partial\sigma_{yy}}{\partial y}+\frac{\partial\sigma_{zy}}{\partial z}=0\\&\frac{\partial\sigma_{xz}}{\partial x}+\frac{\partial\sigma_{yz}}{\partial y}+\frac{\partial\sigma_{zz}}{\partial z}-\rho g=0\end{aligned} \qquad (9)$$

2.3 (d) Compatibility equations

In terms of compatibility equations, one has

$$\frac{\partial^2 \varepsilon_{xx}}{\partial y\,\partial z} = \frac{\partial}{\partial x}\left(-\frac{\partial \varepsilon_{yz}}{\partial x} + \frac{\partial \varepsilon_{zx}}{\partial y} + \frac{\partial \varepsilon_{xy}}{\partial z}\right)$$

$$\frac{\partial^2 \varepsilon_{yy}}{\partial z\,\partial x} = \frac{\partial}{\partial y}\left(-\frac{\partial \varepsilon_{zx}}{\partial y} + \frac{\partial \varepsilon_{xy}}{\partial z} + \frac{\partial \varepsilon_{yz}}{\partial x}\right)$$

$$\frac{\partial^2 \varepsilon_{zz}}{\partial x\,\partial y} = \frac{\partial}{\partial z}\left(-\frac{\partial \varepsilon_{xy}}{\partial z} + \frac{\partial \varepsilon_{yz}}{\partial x} + \frac{\partial \varepsilon_{zx}}{\partial y}\right) \quad (10)$$

$$2\frac{\partial^2 \varepsilon_{xy}}{\partial x\,\partial y} = \frac{\partial^2 \varepsilon_{xx}}{\partial y^2} + \frac{\partial^2 \varepsilon_{yy}}{\partial x^2}$$

$$2\frac{\partial^2 \varepsilon_{yz}}{\partial y\,\partial z} = \frac{\partial^2 \varepsilon_{yy}}{\partial z^2} + \frac{\partial^2 \varepsilon_{zz}}{\partial y^2}$$

$$2\frac{\partial^2 \varepsilon_{zx}}{\partial z\,\partial x} = \frac{\partial^2 \varepsilon_{zz}}{\partial x^2} + \frac{\partial^2 \varepsilon_{xx}}{\partial z^2}$$

3. NUMERICAL SIMULATIONS

3.1 ASSUMPTIONS

The transient temperature field generated during the line heating process was determined based on the physics of heat conduction. The assumptions made for the simulation during the line heating include the followings:

- The material was elastic, perfectly plastic, homogeneous, and isotropic and obeyed the Von Mises yield criterion.
- The metal plate was initially stress-free.
- Heat generated by the plastic and phase transition was small and ignored.
- The temperature field was assumed not affected by the structural response so that the thermal and structural problems could be solved sequentially- with the results of the former used as input to the latter.
- The initial and ambient temperatures of metal plates were the same.
- Heat conduction within the specimen and free convection between the surfaces of the specimen and the surrounding air were considered, but thermal radiation was neglected.

3.2 MODEL AND MESH

The Numerical simulations were carried out with engineering simulation software ANSYS. Simulation of the line heating process was realized by conducting a thermal structure analysis, see Zhou et al. (2009 and 2013). The thermal problem was solved first with the 3D heat conduction equation to establish the temperature field, which was then used as thermal loading for mechanical calculation next. The numerical model of the steel plates was meshed as shown in Figure 4. To resolve the high temperature gradients and stress gradients in the heat-line area, the minimum element length was set to 3~6 mm in the surface plane and 3mm in the thickness direction. To reduce the run times, coarse meshes of 30 mm were used areas away from the heated areas, and transition elements were created to connect the fine and coarse mesh. The full model used for both the thermal and mechanical simulation consisted of approximately 4599 nodes and 3392 elements.

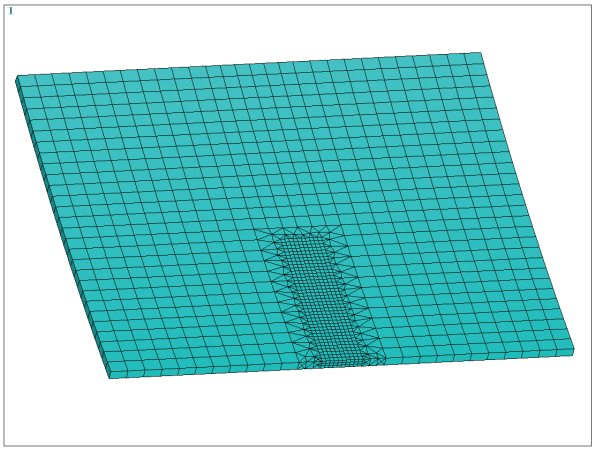

Figure 4. Numerical model of steel plate

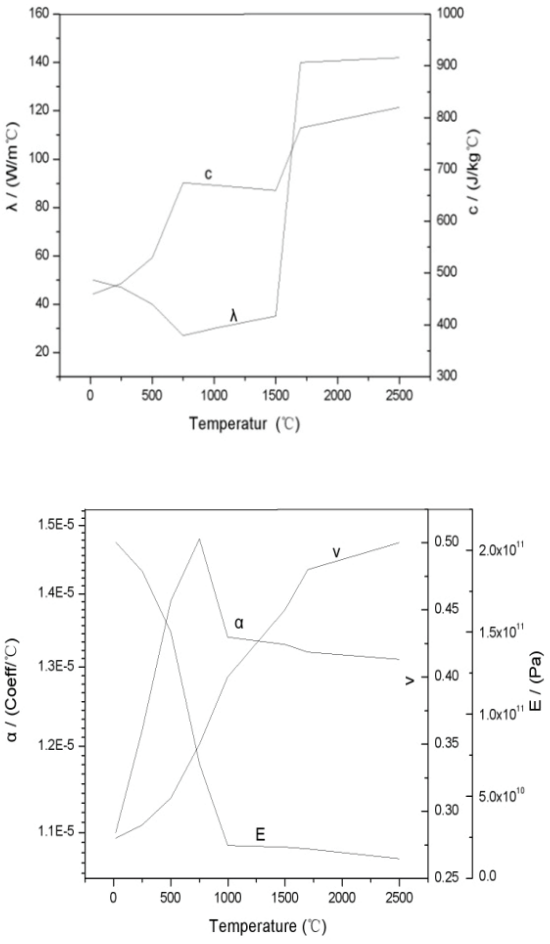

Figure 5. Material properties of carbon steel

3.3 MATERIAL PROPERTIES

The material was mild steel plate which was typical shipbuilding material. As the maximum temperature of line heating process was around 750 degrees Celsius, material properties such as thermal conductivity, specific heat, elastic modulus, yield stress were all temperature dependent. These properties are shown in Figure 5.

3.4 THERMAL BOUNDARY CONDITION

3.4 (a) Gaussian heat source model

A moving body of heat source of Gaussian model (see equation (1)) was used in a finite element simulation of a line-heating process. Figure 6 shows the loading diagram of the heat flux in a single heating line. $R-\theta-z$ is the cylindrical coordinate system for the steel plate; o_2 is the heat source center of current load step. In this illustration, the heat source is moved from initial position o_1 to the new position o_2.

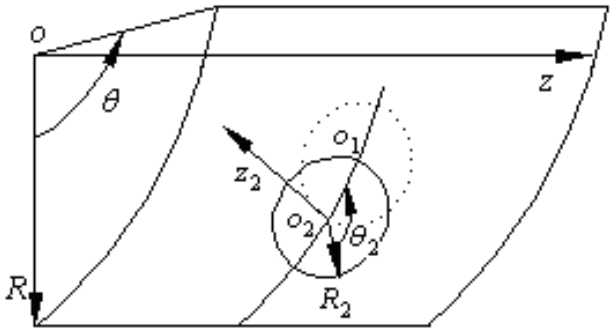

Figure 6. Flux density loading sketch

The heating efficiency η and heating radius r_0 of the Gaussian heat source model could be investigated by combining experiments and numerical simulation, which could be seen in Wang et al. (2006b). In actual line heating process of shipyards, the flows of oxyacetylene and oxygen are basically unchanged. So the parameters of Gaussian heat source are also quite stable. Generally η is in the range of 0.3 to 0.4 and r_0 is in the range of 0.040m to 0.045m.

3.4 (b) Convection heat transfer of water-cooling

In plate forming by line heating, water-cooling is usually used due to its effectiveness in increasing plate deformation. The convective heat in line heating process is so complex that it includes four different regimes: (1) natural or free convection, (2) nucleate boiling, (3) transition boiling, and (4) film boiling. A typical boiling curve for saturated pool boiling of water at atmospheric pressure for a temperature-controlled environment is shown in Figure 6, see Faghri et al. (2010). It could be seen in Figure 7 that the classical pool boiling curve is a plot of heat flux, q", versus excess temperature , ΔT =Tw–Tsat. More discussion about the Convection heat transfer of water-cooling could be seen in Wang et al. 2006. In this study, a trapezoidal area is simplified as a water cooling nozzle region. The distance between the torch and water nozzle is 80 ~ 150mm.

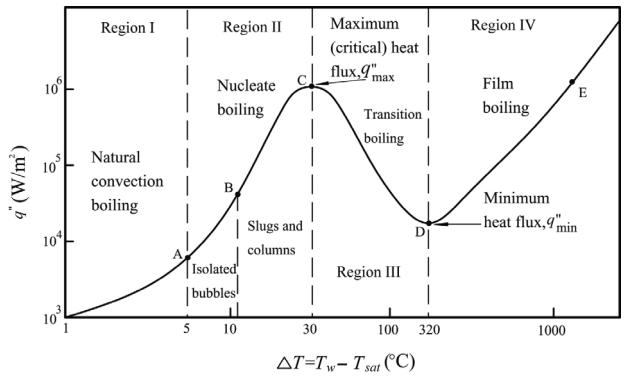

Figure 7. Pool boiling curve for saturated water

3.4 (c) Radiation and air convection heat transfer

Free convection and radiation boundary conditions were satisfied on all surfaces:

$$q = b(T - T_0),$$

$$q = R_r((T - T_Z)^4 - (T_0 - T_Z)^4),$$

3.5 MECHANICAL BOUNDARY CONDITIONS

In the mechanical analysis and to avoid the rigid body movement, boundary conditions were set to zero displacement at endpoints of the metal plate central line (as shown in Figure 8).

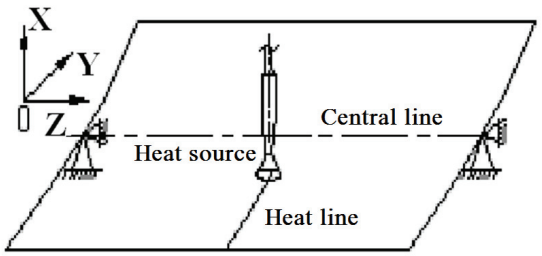

Figure 8. Shell concave plate support

3.6 EXPERIMENT VALIDATION OF THE NUMERICAL MODEL

To validate the numerical model, experiments were conducted as shown in Figure 9. Relevant heating parameters for experiment and numerical simulation are

shown in Table 1. The length of heat lines was 300mm. Process time were 100s, 120s, 150s and 215s, respectively.

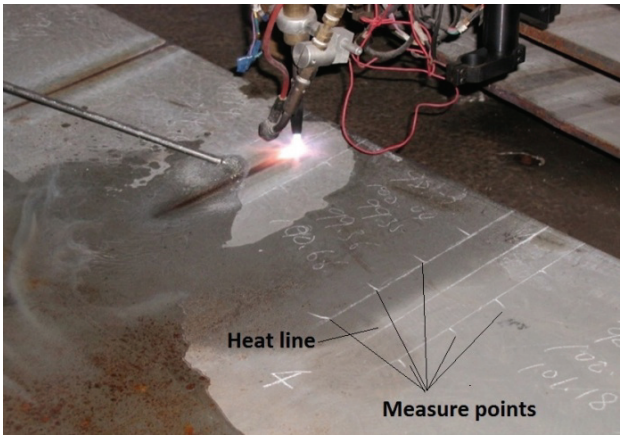

Figure 9. Line heating experiment on curved plate

Table 1. Heating parameters for experiment and numerical simulation

Scheme	1	2	3	4
Time (s)	100	120	150	215
Length (mm)	300	300	300	300

4. RESULTS AND DISCUSSIONS

4.1 TEMPERATURE DISTRIBUTION

The temperature distribution of line heating can be displayed in different ways. The method that was used to display the data in this analysis is the isothermal contours (regions of equivalent temperature). Figure 10 shows the isothermal contours of the numerically simulated temperature distribution on the top-face of steel plate at the heating time of 25.6s, 52.1s, 90.3s and 105s, respectively. Figure 11 shows the variation of temperature with thickness of the sample. The isothermal contour consists of several bands with the temperature increasing from the outer edges to the center of heating line. The part in the middle of the map is the high temperature zone.

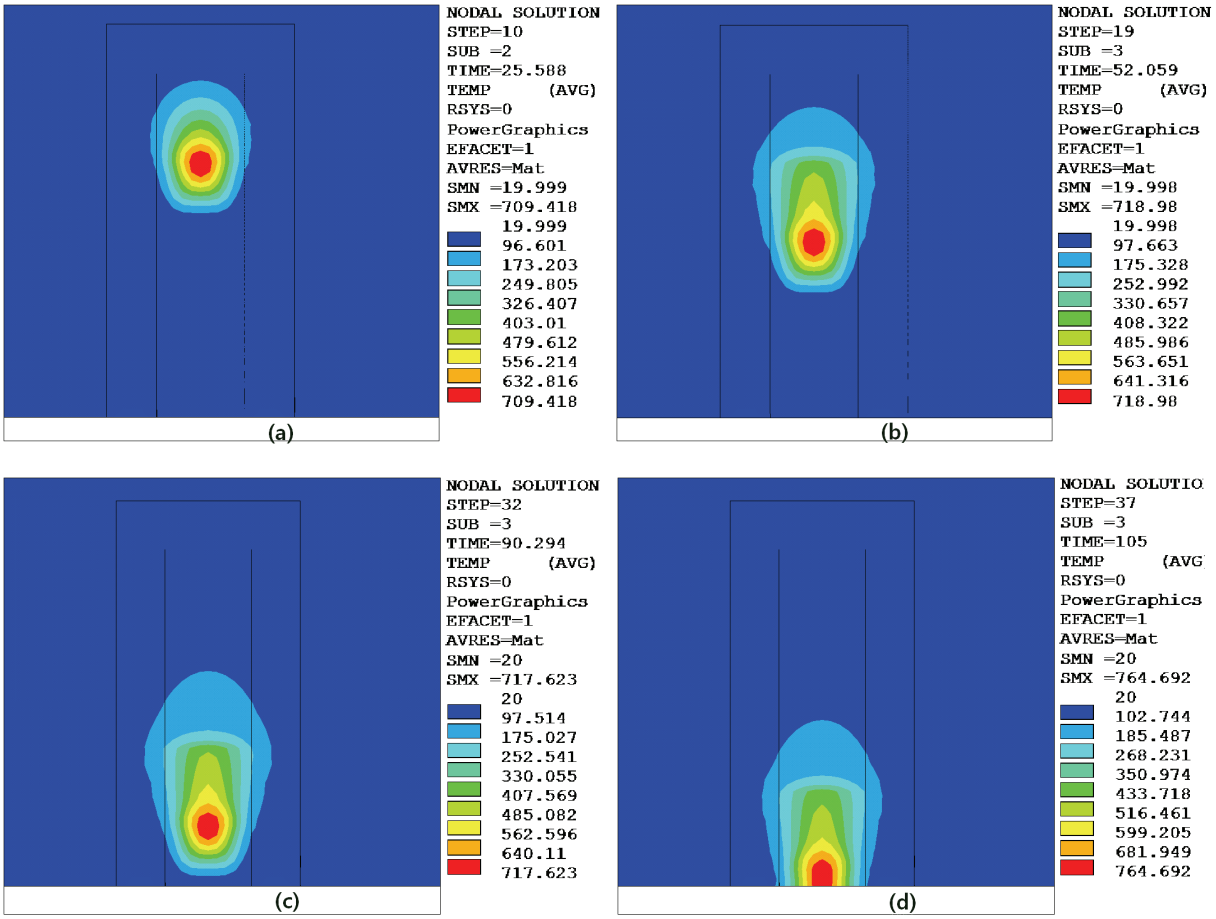

Figure 10. Numerical temperature fields at different moments ((a) t=25.6s; (b) t=52.1s; (c) t=90.3s; (d) t=105s)

It can be seen from Figure 10 and Figure 11 that the distribution of the temperature field changes as the heat source moves along the plate. At the middle of the workpiece, the distribution of the temperature field goes into a quasi-steady state. The isotherm line shows an elliptical shape. The isotherm line is denser in front of the moving thermal source, and the temperature gradient is greater there. But at the back of the moving thermal source, the feature of the isothermal distribution is the reverse of that in front of the moving source.

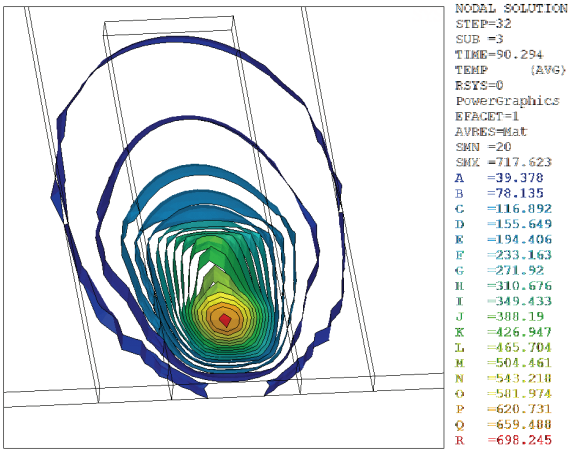

Figure 11. Isothermal surface at 90.3s

Nine test points on the top surface are selected. Among them, three points are in the centre of the heating line, which are the locations at distances of 60, 104 and 148 mm from the start notch. The other six points are perpendicular to the heating line, which are the locations at distances of 0, 8.8, 17.6, 26.4, 35.2 and 44 mm from the centre line. Figure 12 shows the transient temperature history of each point. Workpiece conduction along heating line direction transports thermal energy to each measurement location as the torch approaches. The temperature reaches a peak value as the torch spot passes the plane of the measurement location, and subsequently decays, largely due to conduction of energy from the heated surface.

It could be seen in Figure 10-12 that the temperature of top surface behind heating torch drops quickly due to the effect of water cooling. It could be concluded that the numerical model presented in this paper could model the steady state temperature field of the line heating process at certain heating speed as elaborated herein.

In order to correct heat source model of the finite element analysis, experiments were conducted. Infrared thermography system is a convenient, accurate, non-contact method for making temperature field measurement. The system was used to capture the cutting temperature field, see Huang et al. (2007). The infrared image is show in Figure 13. The temperature distribution of the plates being cut can be displayed in a number of different ways. The method that was used to display the data in this analysis was the isothermal contours (regions of equivalent temperature). The temperature fields measured experimentally at the end of line heating, in the form of isothermal maps from infrared images are shown in Figure 14. The isothermal contour consists of several bands with increasing temperature from the outer edges to the center of heat line. The isotherm shows an elliptical shape and is denser at the leading edge of the moving thermal source. The temperature gradient is greater there. At the tail of the moving thermal source, the converse feature is observed.

It can be seen from Figure 15 that most of the numerical results are within 5% of the experimental results. The excellent match in the overall trends and peak values provides proof that the numerical model for the thermal problem is valid and could simulate the line heating process very well. The proposed model is useful and has a precision that meets the engineering requirement.

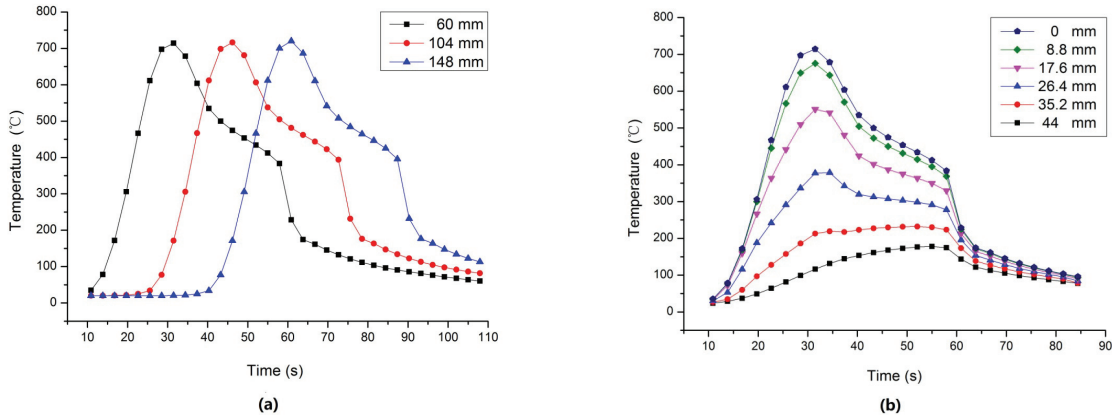

Figure 12. Transient temperature history of test points ((a): Test points along heating line; (b): Test points perpendicular to the heating line)

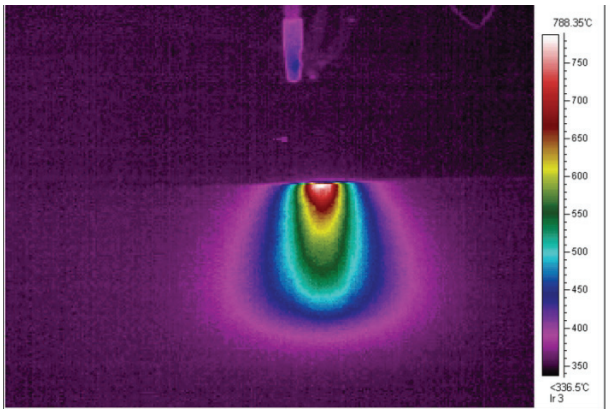

Figure 13. Infrared image of line heating

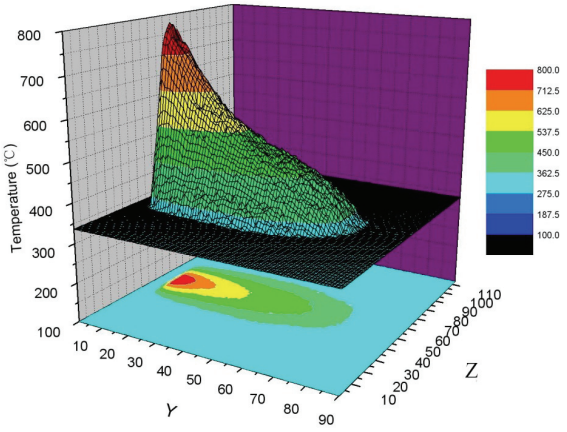

Figure 14. Measured temperature field of line heat experiment

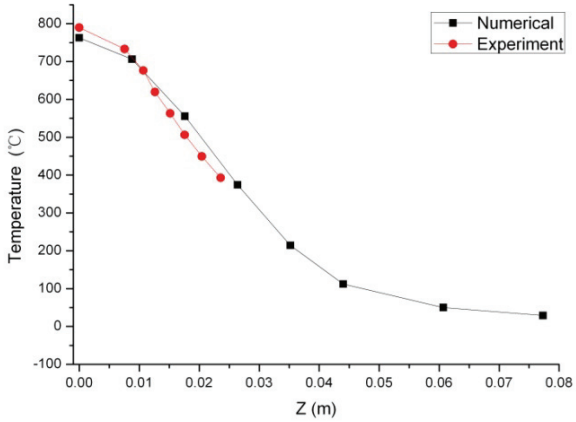

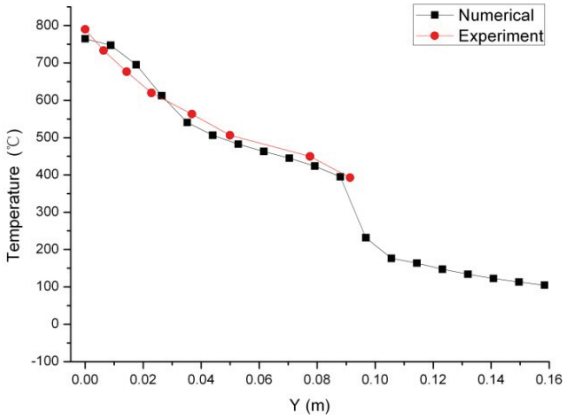

Figure 15. Comparison of the measured and simulated results

4.2 DISTRIBUTION OF RESIDUAL DEFORMATION

The layout of the measurement points is shown in Figure 9 and Figure 14. The displacement between points on the both side of the heat line was taken as the final surface shrinkage. A typical Distribution of residual UZ deformation is shown in the Figure 15. Numerical results were compared with measured results to verify the reliability of the FEA model and the results are shown in Table 2. From Table 2, it could be seen that most of the results were close to one another. The shrinkage curves in the direction of the heating line of Schemes 3 are shown in Figure 15.

It can be seen that most of numerical results agreed well with the experimental results with a variation of 5–10 per cent. From the engineering perspective, it can be concluded that the shrinkages results of all the heat lines are basically the same.

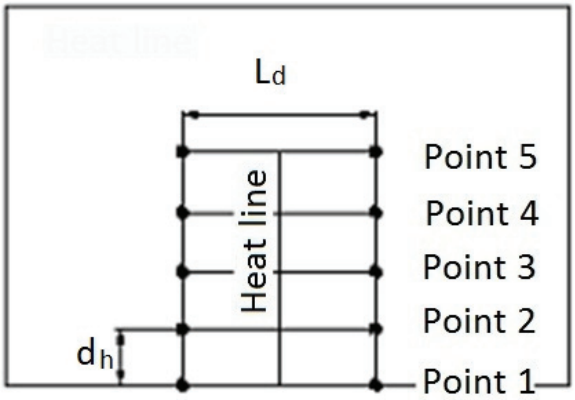

Figure 14. Measurement position on the plate (local surface shrinkage)

4.3 RESIDUAL STRESS DISTRIBUTION

Figure 17 plots the isothermal contours of residual SY stress and residual SZ stress, respectively. Line heating resulted in heating (expansion) and cooling (contraction) of the steel plate. The longitudinal residual stress developed from longitudinal expansion and contraction. Along the heat-line, a high tensile residual stress arises near the heat line, and then decreases to zero, finally becoming compressive, further away from the heat line. From the residual stress contours in Figure 17, one can see that the stress distribution is regular in the heat line area.

Table 2 Experimental measurements and numerical results of surface shrinkage (mm)

Point No.	Scheme 1		Scheme 2		Scheme 3		Scheme 4	
	Measured	Computed	Measured	Computed	Measured	Computed	Measured	Computed
1	0.21	0.186	0.40	0.374	0.80	0.771	1.37	1.498
2	0.24	0.205	0.35	0.335	0.64	0.603	1.14	1.096
3	0.25	0.225	0.30	0.322	0.54	0.496	0.77	0.816
4	0.19	0.198	0.29	0.270	0.40	0.386	0.61	0.599
5	0.10	0.117	0.18	0.153	0.22	0.211	0.37	0.314

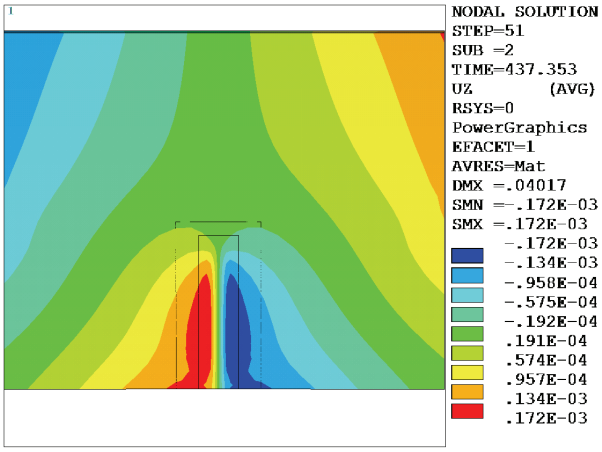

Figure 15. Residual UZ deformation

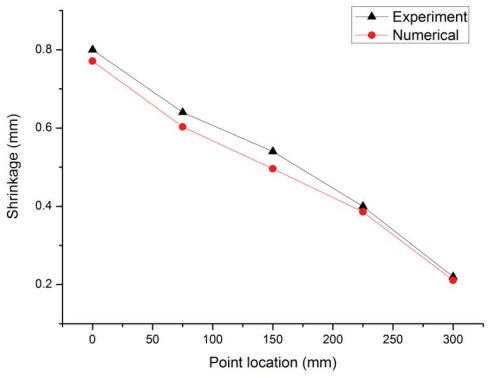

Figure 16. Shrinkage curves in the direction of the heating line for Schemes 3

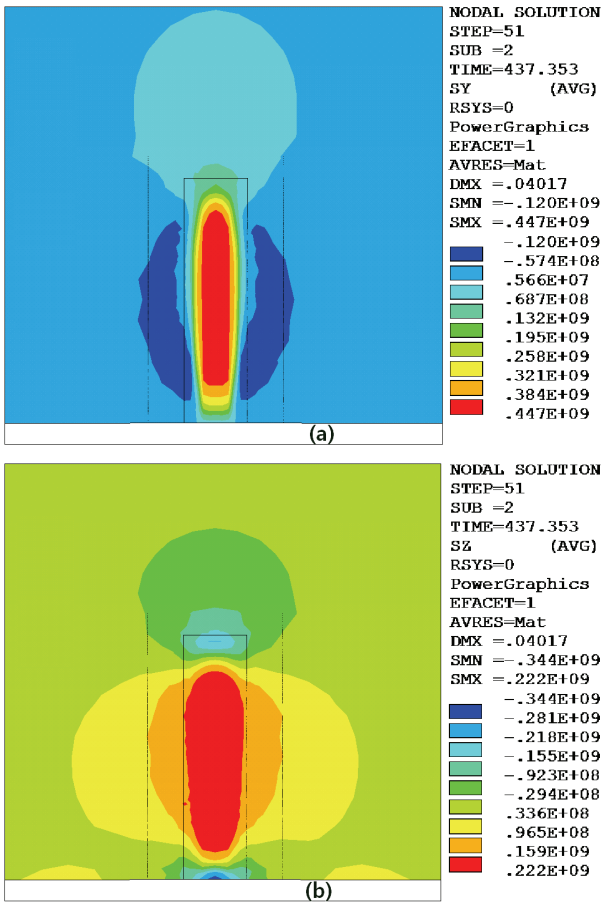

Figure 17. Residual Stress distribution of line heating ((a): SY stress; (b): SZ stress)

In experiment stress analysis, the residual stress is established using the impact-indentation stress measurement method, see Lin et al. (2005). The change in strain, the so-called overlap strain increment, caused by an indentation was measured using a biaxial strain-gage Type BE120-3BA, as shown in Figure 18.

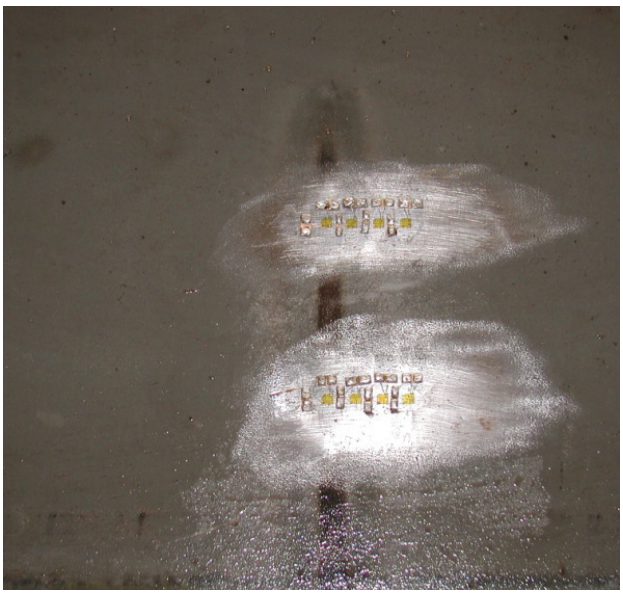

Figure 18. Strain-gage setup

Figure 19 depicts the distribution of residual stress in the X-direction on the top surface, as measured by using the impact-indentation method and the simulated results using the finite element method.

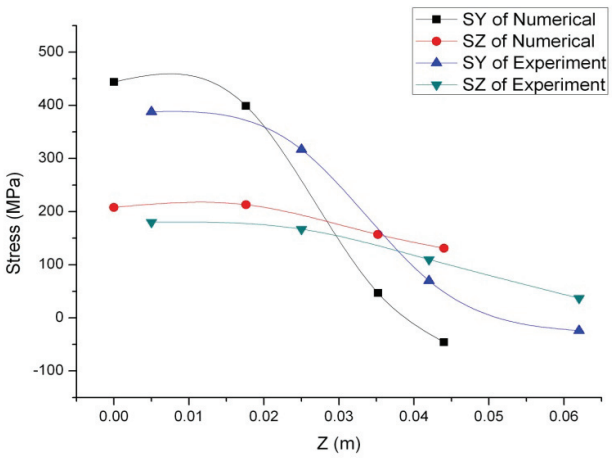

Figure 19. comparison of longitudinal residual stress along the X direction

As can be seen in Figure 19, the simulated results depicted a slight incremental stress compared to the experimental results some distance away from the heat-line, but were almost identical near the heat line area. However, it is also seen that beyond the peak temperatures, the simulated SY stress along the z-direction decrease faster than the measured stress. Despite this discrepancy, the simulated and measured residual stress distributions agreed very well.

4.4 SUMMARY

Several causes can contribute to the discrepancy between the numerical and experimental results, including the coefficient of heat absorption, which is temperature dependent and cannot be make certain, initial temperature of the metal plate is different, the metal plate was not initially stress-free and some other basic assumptions, etc. But from the numerical and experimental results of temperature field, deformation distribution and residual stress distribution, it proves the validity of the numerical model developed for the thermal problem.

5. CONCLUSIONS

The following conclusions can be drawn from the present investigations.

- Through the investigation of basic mechanism and complicated heat transfer condition for line heat process, a numerical thermo-mechanical model was developed and successfully compared with the experimental results.
- The temperature distributions obtained through the numerical analysis and those obtained from experimental measurements compared fairly well with a variation of only 5 per cent for the peak temperatures.
- The shrinkages obtained through the numerical analyses and those obtained from experimental measurements compared fairly well with a variation of 5–10 per cent only. The simulated and measured residual stress distributions also agreed well.
- As the numerical model proposed in this paper is accurate enough to meet the requirement of engineering precision, a serial of numerical experiment could be performed to build up a processing database for the automated line heating control system. It is an effective and economic method instead of doing all the experiment on real steel plates. The proposed method presents a valuable reference for the study of similar thermal process.

6. ACKNOWLEDGEMENTS

The authors acknowledge the support of the CAM Lab, Department of Naval Architecture, Dalian University of Technology, Dalian, China.

7. REFERENCE

1. FAGHRI, A., ZHANG, Y., AND HOWELL, J. R., Advanced Heat and Mass Transfer, *Global Digital Press, Columbia, MO. Page 667*, 2010.
2. JANG, C. D., SEO, S., AND KO, D. E. A study on the prediction of deformations of plates due

to line heating using a simplified thermal elasto-plastic analysis. *Journal of Ship Production, 13(1):22-27*, 1997.

3. JI, Z.S; LIU, Y.J., Development of study of ship hull plate banding by line heating. *Journal of Dalian University of Technology, V 41, n 5, 505-510,* 2001.
4. JONG, G. S., JONG, H. W. Analysis of Heat Transfer Between the Gas Torch and the Plate For the Application of Line Heating. *Journal of Manufacturing Science & Engineering, Vol. 125 Issue 4, p794,* 2003.
5. KITAMURA, N., SAKAI, Y., MURAYAMA, H. 3-Dimensional line heating system for Curved shell plate for shipbuilding, *Technical report, NKK Tsu Laboratories, 1 Kokan-cho Kumozu, Tsu, 514-03 Japan,* 1996.
6. KYRSANIDI, A.K., KERMANIDIS, T.B., PANTELAKIS, .S.G. Numerical and experimental investigation of the laser forming process. *Journal of Materials Processing Technology;87:281–290*, 1999.
7. LIN Q.H., CHEN H.N., CHEN J., LIANG Y.. Residual Stresses Measurement Using an Indentation Made by an Impact Load, *Materials Science Forum, 490, 196–201*, 2005.
8. LIU, Y.J.; GUO, P.J., JI, Z.S., DENG, Y.P. Investigations of technique parameter prediction method of line heating based on genetic algorithm. *Journal of Dalian University of Technology, V 46, n 2, p235-2409*, 2006.
9. MOSHAIOV, A. AND VORUS, W. S. The mechanics of the flame bending process: Theory and applications. *Journal of Ship Research, 31(4):269-281*, 1987.
10. MOSHAIOV, A. AND SHIN, J. G. Modified strip model for analyzing the line heating method-part 2: Thermo-elastic-plastic plates. *Journal of Ship Research, 35(3):266-275*, 1991.
11. OGAWA, J., KAMICHIKA, R., ISAO, N. A simulation on the thermo-elastic-plastic deformation of induction heated steel plate. *ICCAS 94, 8th International Conf on Computer Applications in Shipbuilding, pp. 3.29-3.44(vol.1); Bremen, Germany 5-9*, 1994.
12. ROSENTHAL D. Theory of moving source of heat and its application to metal treatments. *Transactions of American Society of Mechanical Engineers 1946, 68: 849-866*.
13. RYKALIN, N.N., Calculation of Heat processes in Welding, *Mashinotroenije, Moscow*, 1960.
14. ZIENKIEWICZ O.C., TAYLOW R.L. The Finite Element Method, fifth ed., *Solid Mechanics, vol. 2, Butterworth-Heinemann, Oxford, UK*, 2000.
15. SHIN, J.G., RYU, C.H., LEE, J.H., KIM W.D. User-friendly, advanced line heating automation for accurate plate forming. *Journal of Ship Production, 2003, 19(1):8-15*, 2003.
16. UEDA K., MURAKAWA H., RASHWAN A. M., OKUMOTO Y., AND KAMICHIKA R. Development of computer-aided process planning system for plate bending by line heating (report 1) – relation between final form of plate and inherent strain. *Journal of Ship Production, 10(1):59-67*, 1994.
17. UEDA K., MURAKAWA H., RASHWAN A. M., OKUMOTO Y., AND KAMICHIKA R. Development of computer-aided process planning system for plate bending by line heating (report 2) – practice for plate bending in shipyard viewed from aspect of inherent strain. *Journal of Ship Production, 10(4):239-247*, 1994.
18. UEDA, K., MURAKAWA, H., RASHWAN, A. M., OKUMOTO, Y., AND KAMICHIKA R. Development of computer-aided process planning system for plate bending by line heating (report 3) – relation between heating condition and deformation. *Journal of Ship Production, 10(4):248-257*, 1994.
19. WANG, J.，LIU, Y.J., JI, Z.S., DENG, Y.P., ZHANG J., 2006a. Study on forced convection boundary condition for subcooled water in the simulation of line-heating process. *Journal of Ship Production, 22(1): 41-47*.
20. WANG, J.，LIU, Y.J., JI, Z.S., DENG, Y.P., 2006b. Investigation on parameters of heat input model in numerical simulation of line heating, *Journal of Dalian University of Technology, 46 (3)：367-371*.
21. YU, G, MASUBUCHI, K., MAEKAWA, T., PATRIKALAKIS, N.M. A finite element model for metal forming by laser line heating. *In: Chryssostomidis C, Johansson K, editors. Proceedings of the 10th International Conference on Computer Applications in Shipbuilding, ICCAS '99, vol. 2. Cambridge, MA: MIT,. p. 409–18*, 1999.
22. YU, G. Modeling of shell forming by line heating. *Ph.D. thesis, Massachusetts Institute of Technology, Cambridge, MA*, 2000.
23. YU, G., ANDERSON, R.J., MAEKAWA, T., PATRIKALAKIS, N.M. Efficient Simulation of Shell Forming by Line Heating. *International Journal of Mechanical Sciences 43,* 2001.
24. ZHOU, B., LIU, Y.J., JI, Z.S. Numerical and experimental investigations on Temperature and stress distribution in oxygen cutting. *Journal of Ship Production, 25(1): 14-20*, 2009.
25. ZHOU, B., LIU, Y.J., TAN S.K. Efficient simulation of oxygen cutting using a composite *Heat and Mass Transfer, 57, 304–311*, 2013.